Flexible symmetric and asymmetric supercapacitors based in nanocomposites of carbon cloth/polyaniline - carbon nanotubes

M.A. Bavio [a, *], G.G. Acosta [a], T. Kessler [b, 1], A. Visintin [c]

[a] INTELYMEC (UNCPBA), CIFICEN (UNCPBA-CICPBA-CONICET), Av. del Valle 5737, B7400JWI Olavarría, Argentina
[b] Facultad de Ingeniería, UNCPBA, Av. del Valle 5737, B7400JWI Olavarría, Argentina
[c] INIFTA, UNLP-CONICET, Facultad de Ciencias Exactas, CC. 16, Suc. 4, 1900 La Plata, Buenos Aires, Argentina

ARTICLE INFO

ABSTRACT

This paper describes the construction of flexible symmetric and asymmetric supercapacitors made of carbon cloth, polyaniline and carbon nanotubes. The electrode materials (nanostructures of polyaniline-carbon nanotubes, PANI-CNT) were supported on carbon cloth acting as current collector. PANI-CNT nanostructures were synthesized through an oxidative polymerization process in the monomer (aniline) acid solution with the presence of a surfactant and the addition of multi-walled CNT. The CNT were used with and without pretreatment. The cells electrolyte was H_2SO_4 0.5 M and the selected potential range was 1 V. In order to test their behavior, the different cells configurations were evaluated by electrochemical techniques. Polyaniline nanostructures and polyaniline-carbon nanotubes nano-composites were used to make the negative and/or positive electrodes of the cell. The cathode in the asymmetric supercapacitors was always carbon cloth/carbon black. The behavior of the arrayed super-capacitors was evaluated by cyclic voltammetry, between 0.0 and 1.0 V at different scan rates (10 -100 mVs^{-1}), as well as with galvanostatic charge/discharge runs at current densities between 0.3 and 6.7 mAcm^{-2}. At a constant current density of 0.3 mA cm^{-2}, a specific capacitance value of 1275 Fg^{-1} was obtained for a symmetric assembly using both electrodes prepared with polyaniline and carbon nano-tubes nanocomposites. When the set was asymmetric, being the positive electrode made of polyaniline and carbon nanotubes nanocomposites, the specific capacitance value was 1566 Fg^{-1}. For the latter array, the specific power and energy density values were 125 Wkg^{-1} and 217 Whkg^{-1} at 0.25 Ag^{-1}, and 2502 Wkg^{-1} and 71 Whkg^{-1} at 5.0 Ag^{-1}. These results suggest a good energy transfer capacity. Moreover, symmetric and asymmetric supercapacitors demonstrated a high stability over 1000 cycles obtaining a capacitance retention of more than 85%.

1. Introduction

Energy and the environment are indispensable for sustainable development. The demand for environmental resources, especially water, food and fuel, has grown as drastically increases population and consumption rate.

Industrial and technological development and the use of energy are intimately linked. In fact a key problem for the next few years is how to ensure sufficiently reliable and economical energy sources that guarantee us an adequate level of development. At present, research tends to develop and incorporate new technology to increase the energy efficiency of current processes and incorporate renewable sources such as biomass, wind, solar, electrochemical energy systems [1,2].

The solar and wind energy are less contaminant and more friendly to the environmental, but requires to energy storage systems due to are unstable and intermittent [3].

The batteries offer a storage solution based on chemical processes. This fact can be decisive for key issues, such as price (due to its components), limitation of loading and unloading capacity and limitation of the number of cycles of use. In recent times super-capacitors have been used to store electrical energy based on physicochemical processes. Supercapacitors, unlike batteries, have high cycling, low maintenance costs, high power and can operate in extreme temperatures [4,5].

Studies have recently been carried out in which both

technologies complement. Examples of these are electric powered vehicles or autonomous mobile robots. The batteries would provide most of the energy needed for the vehicle in while the supercapacitors would be responsible for necessary power in slopes or overtaking; absorb the peaks of kinetic energy in the braking; or to power the starter motor at startup [6,7].

In recent years electronics has developed considerably tending to be flexible and portable. In this way, energy storage devices that are flexible, small and light must be developed. Supercapacitors are the best alternative for these types of flexible electronic devices. The main requirements for them are flexible and low-weight electrodes and membrane/electrolyte system [8—10].

As electrode active materials a variety of single or mixed oxides, carbonaceous materials, or conductive polymers have been used [11]. In different configurations, symmetrical or asymmetrical, several metal oxides have been used, among them, Bi_2O_3 [12], MnO_2 [13], NiO [14], Mn_3O_4 [15], RuO_2 [16], Co_3O_4 [17]. Have high specific capacities and electrical conductivities and are easily processable, with a dominant pseudocapacitive or redox type mechanism.

On the other hand, carbonaceous materials such as activated carbons, carbon black, carbon nanotubes, graphene, graphene oxide. These materials presents a capacitive charge/discharge, high conductivities and specific surface and some have low cost [18—21].

Finally, the most used conductive polymers are polythiophene, polypyrrole, polyaniline and their derivatives. Its main features include a pseudocapacitive loading/unloading mechanism, a moderate specific surface, electrical conductivities and specific high capacities [22,23].

Nanostructured hybrid materials have recently been developed to be used as electrode materials in supercapacitors, the advantage is the combination of a double layer loading mechanism and a redox mechanism. In this way values of capacitance, energy and high powers are obtained. Nanocomposites of conducting polymers or metal oxides (with pseudocapacitive mechanism) and carbonaceous materials (double layer mechanisms) are promising for supercapacitors [24—27].

In previous studies our group showed that nanocomposites of polyaniline and carbon black or carbon nanotubes can be used as electrode materials in supercapacitors [28,29]. Other researchers have also reported several values of specific capacitance of PANI (polyaniline) nanostructures from 200 to 2300 Fg^{-1}, with different particle size, the synthesis method, porosity and experimental conditions [23,30], and reported capacitances values between 200 and 600 Fg^{-1} when used PANI-CNT nanocomposites [31,32].

Different prototypes of flexible supercapacitors were development using films of carbon black/graphene as electrodes materials and membranes of polyvinylalcohol/H_2SO_4 system as the electrolyte/separator [33]. A symmetric configuration was presented using current collector support and flexible steel mesh, with commercial ink as electrodes [34]. Printable and flexible supercapacitors based on activated carbon and gel electrolyte were developed [35]. Polypyrrole/graphene oxide/zinc oxide was used like electrodes materials in flexible symmetric supercapacitor by sandwiching in a PVA hydrogel polymer electrolyte [24].

In this work, the construction of flexible symmetric and asymmetric supercapacitors using polyaniline nanostructures and polyaniline-carbon nanotube nanocomposites over carbon cloth as electrode materials is presented. The capacitive behavior is evaluated by electrochemical techniques, analyzing capacitance values, specific energy, power, and stability with repeated cycles of charge/discharge. In this paper, we demonstrate that flexible symmetric and asymmetric supercapacitors provide increased capacitance and specific energy and can be fabricated easily.

2. Experimental

2.1. Nanocomposites as electrode materials

In previous work the synthesis and characterization of PANI nanostructures and PANI-CNT functionalized or not functionalized was presented. The functionalization process was carried out by an oxidizing pretreatment with nitric acid. CNT were treated in 2.2 M nitric acid. The amount of CNT was 0.85 mg mL^{-1} and the suspension was kept at room temperature for one hour. Then, the preparation was stirred using an ultrasonic bath for 30 min and kept at room temperature for 20 h. Afterwards, it was filtered and washed with abundant distilled water to achieve neutral pH in the filtrate solution. Finally, the treated carbon nanotubes were dried at 37 °C for 2 h [28].

These materials were used to make the negative and/or positive electrodes of the cell. The nanocomposites were synthesized mixing multiwall carbon nanotubes, functionalized (CNTf) or unfunctionalized (CNT), dispersed in aniline and a surfactant, by magnetic stirring at ambient temperature, with subsequent addition of ammonium persulfate. These materials were properly characterized by TEM, SEM, FTIR, UV—Vis and XRD. Complete synthesis method and results were presented in a previous paper [28].

2.2. Construction of electrodes

A dispersion of the materials synthesized in a solution of isopropyl alcohol and distilled water was prepared. The mixture was spread on one side of the carbon cloth (CC) that acts as support and collector current. Afterwards, they were dried at room temperature for 30 min.

Successive depositions were performed until the total material load was 2 mg. Then, a 5% Nafion® solution was added, and again, the electrode was dried at room temperature for the same amount of time. Carbon cloth (plain Excel®) with an expose geometric area of 1.5 cm^2 was used. The back side of the carbon cloth was sealed with a Teflon® fabric adhesive. The electrodes with carbon nanotubes were prepared similarly, using the same load of total material, namely 1.3 mg cm^{-2}. The electrode assembly is shown in Fig. 1.

Electrodes of CC and carbon black (CB) over carbon cloth (CC-CB) were built in the same way. In the first case a 5% Nafion® solution was added over CC, and the electrode was dried at room temperature. For CC-CB, 2 mg of CB were deposit over CC, and then a Nafion® solution was added, keeping the original method.

2.3. Supercapacitor assembly

Symmetric and asymmetric cell configurations with different electrodes as anodes and cathodes were tested, as shown in Table 1. The electrodes and separator (filter paper) were soaked in the electrolyte for 15 min before use in H_2SO_4 0.5 M. Then, the cell was sealed with Teflon® adhesive tape before starting the electrochemical measurements. The cell assembly is shown in Fig. 1. The nomenclature of supercapacitors refers to designs characteristics and the composition of the electrodes. Where: S = symmetric, A = asymmetric, C = carbon clot, B = carbon black, P = Polyaniline, N = Carbon nanotubes, nf = not functionalized and f = functionalized.

2.4. Performance testing of supercapacitors

The performance of the different supercapacitors was evaluated by cyclic voltammetry and galvanostatic measurements. I/V runs were recorded in the potential range of 0.0—1.0 V at various sweep rates, varying from 10 to 100 mVs^{-1}.

Electrodes
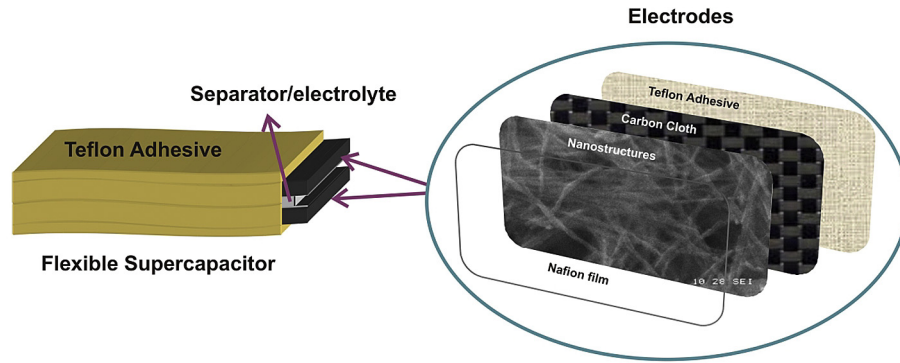

Fig. 1. Electrodes composition and cell assembly.

Table 1
Cells configuration for symmetric and asymmetric supercapacitors.

Nomenclature	Anode	Cathode
S-C	CC	CC
S-CB	CC-CB	CC-CB
A-CB	CC	CC-CB
S-CP	CC–PANI	CC–PANI
S-CPNnf	CC-PANI-CNTnf	CC-PANI-CNTnf
S-CPNf	CC-PANI- CNTf	CC-PANI- CNTf
A-CP	CC–PANI	CC–CB
A-CPNnf	CC-PANI-CNTnf	CC–CB
A-CPNf	CC-PANI- CNTf	CC–CB

The charge/discharge experiences were made at different current density values, between 0.3 and 6.7 Acm^{-2}, in the potential range of 0.0–1.0 V.

The specific capacitance values were calculated from the voltammetric and galvanostatic measurements.

All the electrochemical experiments were performed using a potentiostat/galvanostat EG&G PAR Model 362, coupled to a Nicolet oscilloscope with an acquiring data switch connected to a PC.

The specific capacitance values were calculated from the cyclic voltammograms using the following equation:

$$Cm = \frac{\int_{V_1}^{V_2} I(V)dV}{(V_2 - V_1)\, v \cdot m} \qquad (1)$$

where I is the current in the I/V Profiles, $\int_{V_1}^{V_2} I(V)dV$ is the area under the curve I/V, v is the scanning rate, $(V_2 - V_1)$ is the potential window, m is the mass of the electroactive material.

From the galvanostatic measurements, parameters such as the specific capacitance of the material (Cm), the specific energy (Es), the specific power (Ps) and the coulombic efficiency (η) were calculated, applying by the following equations, (2) to (5), respectively:

$$C_m = 2\frac{C}{m} = 2\frac{I\ \Delta t_d}{\Delta V\ m} \qquad (2)$$

$$E_s = \frac{I\ \Delta V\ \Delta t_d}{m} \qquad (3)$$

$$P_s = \frac{I\ \Delta V}{m} \qquad (4)$$

$$\eta = \frac{\Delta t_d}{\Delta t_c} \cdot 100\% \qquad (5)$$

where C is the experimental capacitance value, I is the charge/discharge current, Δt_d is the download established time, ΔV is the potential range, m is the mass of a composite employed as electrode and Δt_c is the charging time.

3. Results and discussion

3.1. The electrode materials

In previous work [28] it was shown that the addition of CNT to the initial solution promotes the growth of various PANI-CNT nanostructures, depending on the pretreatment of carbon nanotubes. Nanocomposites and nanostructures of PANI present the following properties:

- PANI nanotubes with an average diameter of 95 nm and a length of approximately 10 μm. Trough spectroscopy analysis it was determined that the polyaniline was found to be in the emeraldine salt and doped form, resulting from the use of APS during the synthesis (Fig. 2a).
- PANI-CNTf nanotubes with an average diameter of 92 nm and ca. 12–15 μm wide are shown in Fig. 2b. Nano-wires of 20–25 nm in diameter and 30–40 nm in length grew on the walls nanotubes. By UV–Vis and FTIR analysis it was determined that the polyaniline was doped and in its conductive form of emeraldine salt, due to the use of APS.
- PANI-CNTnf, presents a granular structure as an aggregate of nanoparticles of 95 nm diameter (Fig. 2c).

Polyaniline doped through the use of surfactant, SDS, was found in all nanostructures. This contributes to the doping of the polyaniline chain by electrostatic interactions with the cation anilinium at the beginning of the polymerization, prior to the formation of the supramolecular structure [36,37].

3.2. Cyclic voltammetry

Fig. 3 show the voltammograms of S-C, S-CB and A-CB supercapacitors at different scan rate, these do not exhibit peaks, demonstrating a capacitive behavior. Also the S-C is apparently more resistive than the S-CB and A-CB, due to the aggregation of the carbon black a better electrical conductivity is achieved.

Voltammograms of Symmetric and asymmetric arrangement, at different scan rates, are shown in Fig. 4 (a,b,c) and Fig. 4 (d,e,f),
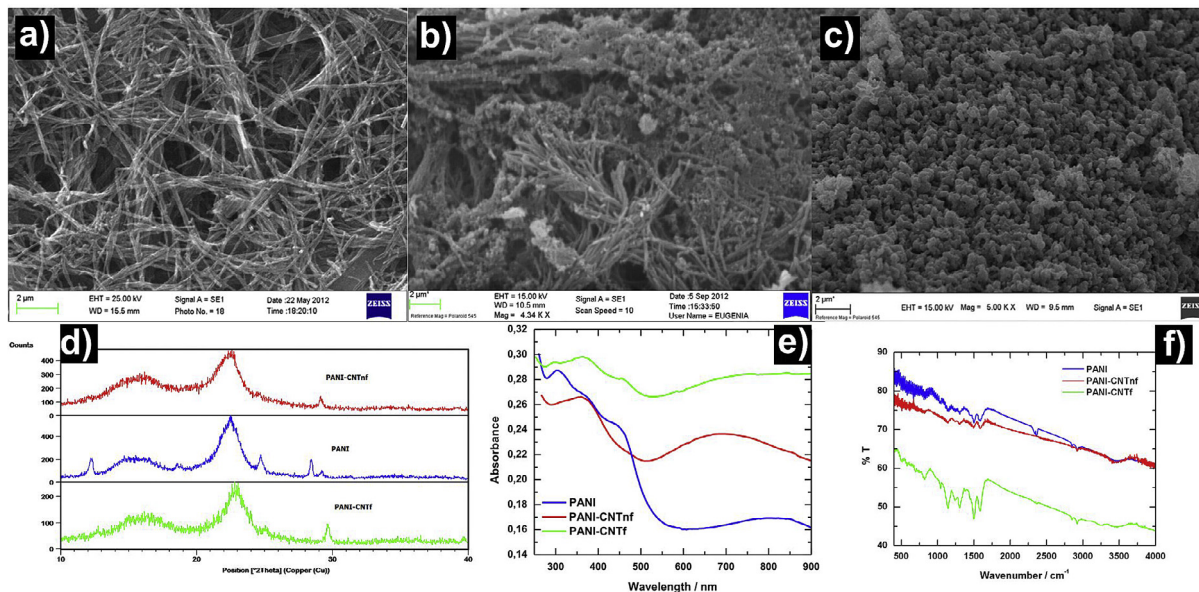
Fig. 2. SEM images of electrode materials. a) PANI, b) PANI-CNTf and c) PANI-CNTnf. d) DRX, e) UV−Vis and f) FTIR.
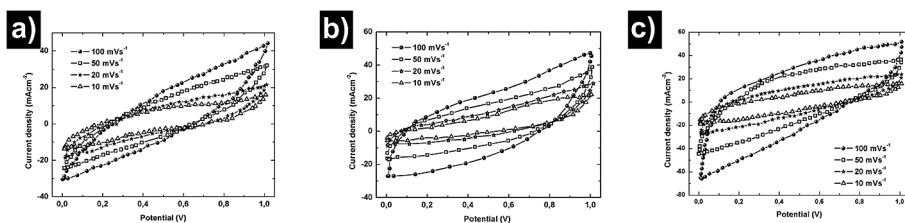

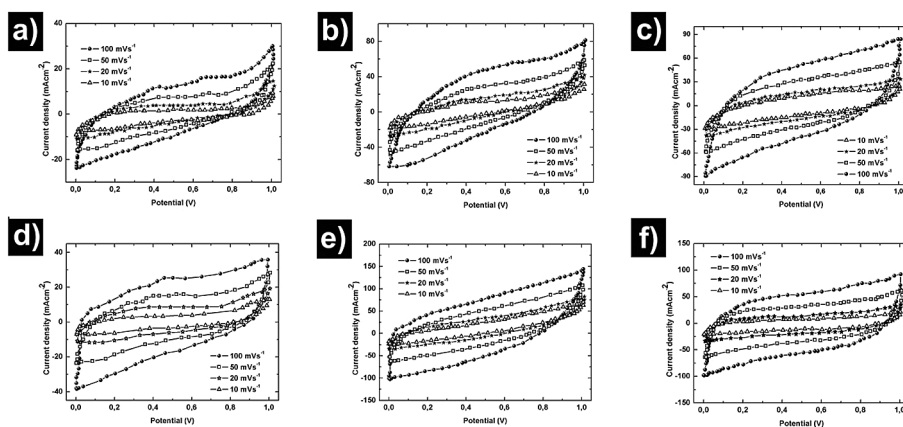**Fig. 3.** Cyclic voltammograms of supercapacitors a) S-C, b) S-CB and c) A-CB at different scan rate (10, 20, 50 and 100 mVs^{-1}).

Fig. 4. Cyclic voltammograms of symmetric and asymmetric supercapacitors at different scan rate (10-100 mVs^{-1}). a) S-CP, b) S-CPNnf, c) S-CPNf, d) A-CP, e) A-CPNnf and f) A-CPNf.

respectively. All voltammograms in Fig. 4 presented high current density and no evident current peaks, indicating good electrochemical activity and high power density. It is to point out that they present an almost capacitive behavior in their voltammograms. Effectively the anodic and cathodic runs are not completely symmetric and rectangular shaped. This fact may be attributed to a pseudocapacitive contribution corresponding to the polyaniline incorporated as electrode material.

In Table 2, specific Capacitance values calculated from the CV measurements are presented. The voltammograms of symmetric and asymmetric assemblies present a current response become larger at increasing sweep-rates. This situation can be attributed to that the electrolyte resistance increases down the linear pores with progressive loss of charging/discharging access. In all supercapacitors the specific capacitance values increases as decreases scan rate. This is due to the fact that at high rates, the measured capacitance simply approaches that of the pore orifice, and it is only as the sweep-rate slows that the signal can "penetrate" into the

Table 2
Specific capacitances obtained by cyclic voltammetry at different scan rate.

Scan rate	Specific Capacitances Fg^{-1}								
mVs^{-1}	S-C	S-CB	A-CB	S-CP	S-CPNnf	S-CPNf	A-CP	A-CPNnf	A-CPNf
10	290	312	346	477	760	1072	485	975	1240
20	282	275	289	436	489	815	447	746	998
50	224	245	256	292	310	569	302	436	826
100	123	197	228	234	273	411	289	387	602

pore, thus giving rise to increased charge acceptance and hence measured capacitance [38].

Comparing the capacitance values for the various asymmetric arrangements, the best results are obtained with electrodes prepared from PANI-CNTf nanocomposites at any scan rate and analogous results were obtained for the symmetric supercapacitors. It is evident that the asymmetric conformation provides higher capacitance values compared to the symmetric assembly. In addition the morphology of the nanocomposites is directly related to the obtained capacitance values. Similar results were obtained in previous work by us with supercapacitors based on polyaniline - carbon black nanocomposites [39] and by Y. Cao group with asymmetric cells of Perovskite-type Lanthanum Cobaltate Nanofibers with Sr-substitution [40]. The maximum specific capacitances at low scan rate were obtained with A-CPNf and S-CPNf assemblies, namely 1240 and 1072 Fg^{-1} respectively.

The electrochemical performance of A-CPNf and S-CPNf were measured under bending conditions at two different angles, 45° and 90°, with the aim to evaluate the potential of the supercapacitors as flexible energy storage devices. Fig. 5 show the voltamperograms of both supercapacitors at 100 mVs^{-1} flexed at 45° and 90°. Clearly, the bending angle does not substantially alters the capacitive properties of supercapacitors.

3.3. Galvanostatic measurements

Fig. 6a) and b) show the galvanostatic charge/discharge curves of symmetric and asymmetric cells configuration at 0.25 Ag^{-1}, respectively.

The asymmetric supercapacitors present a more lineal profile in comparison to symmetric supercapacitors. The voltage drop (IR-drop) during the initial stage of the discharge process in the asymmetric cells is less than in symmetric configuration. Evidently asymmetric supercapacitors have lower internal resistance symmetrical supercapacitors.

Fig. 7 shows the specific capacitances of the supercapacitors in relation to the applied charge/discharge current for symmetric and asymmetric supercapacitors.
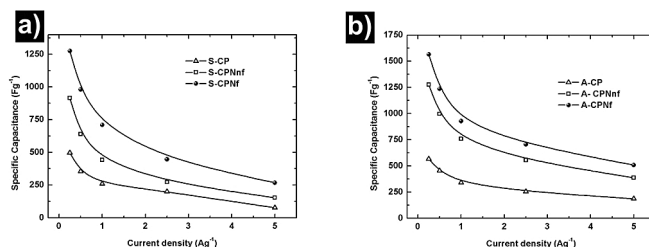
Regardless of the cell configuration, a decrease in the current applied implies an increase in specific capacitance. In symmetric and asymmetric devices, the inclusion of CNTf improves the
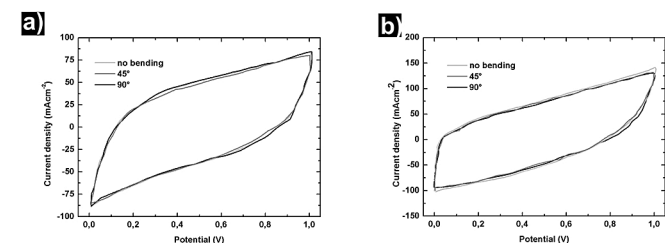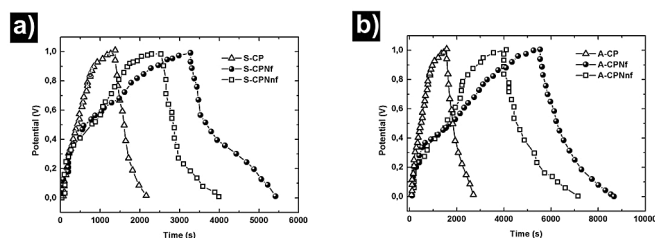
Fig. 6. Galvanostatic charge/discharge curves of a) symmetric and b) asymmetric configuration at current density of 0.25 Ag^{-1}.

Fig. 7. Specific capacitances of the supercapacitors in relation to the applied charge/discharge current for symmetric and asymmetric supercapacitors.
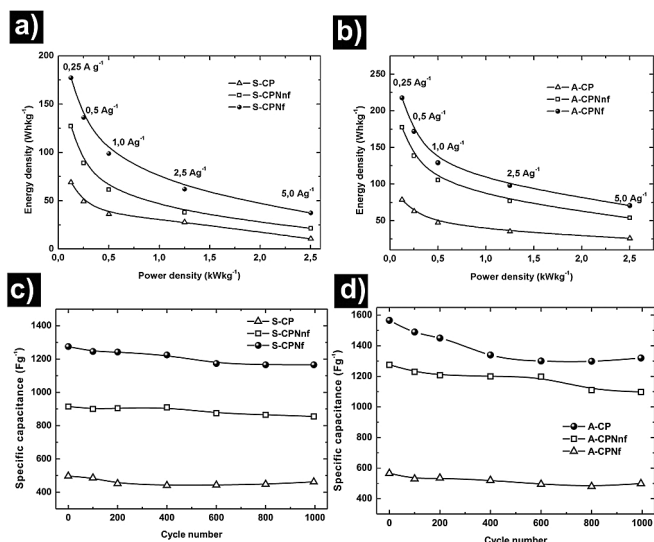
specific capacitance from 566 Fg^{-1} to 1566 Fg^{-1} when comparing A-CP and A-CPNf asymmetric assemblies and from 497 Fg^{-1} to 1275 Fg^{-1} for S-CP and S-CPNf symmetric configuration. These results are comparable with those obtained by cyclic voltammetry.

The special morphology of nanocomposites PANI-CNTf improves specific capacitance values compared to those systems not containing CNTf, being the effect less pronounced. The coexistence of nanorods of PANI over CNT favours the fast penetration of the electrolyte, facilitates ion diffusion, and shortens the charge transfer distance, all of which lead to the superior electrochemical performance of S-CPNf and A-CPNf.

In these designs the presence of carbon cloth, as a current collector and as a carrier, promotes the reduction of the collector-support contact resistance. In addition the incorporation of carbon black in the cathode of the asymmetric supercapacitors allows an increase in the conductivity of electrode/electrolyte interface, which leads to a decrease in the internal resistance, and therefore an increase in the capacitance [2,14].

One of the most significant aspects of the performance of supercapacitors is their capability of delivering power at high power-densities. In addition, the relation of the latter to energy-densities is of significant importance, as revealed by Ragone plots. Fig. 6a) and b) shows these plots as the relationship between the specific energy density and specific power density for the assembled supercapacitors.

Fig. 8 a shows the energy density and power density for symmetric supercapacitors calculated. Thus, while the energy density decreased from 177 to 37 Whkg^{-1} the power density increased

Fig. 5. Voltamperograms under bending conditions of a) S-CPNf and b) A-CPNf supercapacitors at 100 mVs^{-1} flexed at 45 and 90°.

Fig. 8. Ragone plots of a) symmetric and b) asymmetric supercapacitors. Cycles life test of c) symmetric and d) asymmetric supercapacitors measured at 0,25 Ag⁻¹.

from 125 to 2502 W kg^{-1}, for the S-CPNf assembly. The higher specific energy and power values are obtained for asymmetric supercapacitors (Fig. 8b). When the charge/discharge current density is increased from 0.25 to 5 Ag^{-1}, the energy density decreased from 217 to 71 Whkg^{-1} in A-CPNf, but the power density increased from 125 to 2502 Wkg^{-1}. The supercapacitor stability was evaluated over 1000 charge/discharge cycles. In Fig. 6c) and d), the specific capacitances of the supercapacitors are presented as a function of the number of cycles, calculated at 0.25 Ag^{-1}. It was found that the capacitance loss during the charge/discharge process is less than 20% for all the prepared supercapacitors.

Another important parameter to analyze is their coulombic efficiency (η) in relation to the applied current density. Thus, at high current density values (5 Ag^{-1}), all the prepared supercapacitors have a charge/discharge efficiency of ca. 90%. On the other hand, at low current densities (0.25 Ag^{-1}) the symmetric devices maintain a high efficiency, ca. 80%, while for the asymmetric configurations this value falls to ca. 75%. In summary, the incorporation of CNTf in the electrode material improves reatly the performance of the symmetric and asymmetric supercapacitors. This fact can be attributed to introducing carboxylic groups on CNT plays two key roles in improving the performance of CNT capacitors: - it decreases the surface resistivity of CNT, and enhances the surface wettability of CNT, which not only offers more accessible sites for the physisorption of free electrolyte ions on CNT surfaces, but also increases the ionic conductivity at the electrode–electrolyte interfaces [41]. This effect is enhanced in the asymmetric supercapacitors due to the incorporation of carbon black in the anode. In fact the electrochemical parameters for the A-CPNf arrangement are 20% larger than the ones for the S-CPNf assembly. However, all of the constructed devices exhibited a very good stability with a retention capacitance of 85–95%, and an efficiency of 80–90% at high current densities. Similar results were obtained by our group with symmetric and asymmetric supercapacitors based in polyaniline–carbon black nanocomposites [39].

The main advantages in using this type of design is that the supercapacitors were manufactured through a simple method and they are flexible due to the use of carbon cloth and Teflon® adhesive tape, allowing its use as flexible/wearable power sources for next generation in portable electronics.

4. Conclusions

Flexible symmetrical and asymmetrical supercapacitors were constructed using polyaniline nanostructures and polyaniline and carbon nanotubes nanocomposites as electrode. Carbon cloth was used as a current collector and as nanostructured material support, thereby preventing a loss of electrode/current collector junctions. Capacitances values obtained for asymmetric devices are higher in all current densities evaluated, thereby providing increased power and specific energy.

All devices were stable for 1000 cycles of charge/discharge, with a retention capacitance of more than 85%.

Thus, flexible supercapacitors, of low weight and with high capacitances, power and energy, were designed. Therefore, these characteristics made them suitable for application in portable electronic devices.

Acknowledgments

References

[1] Kothari DP, Singal KC, Ranjan R. Renewable energy sources and emerging technologies. India: PHI Learning Private Limited; 2008.

[2] Kim BK, Sy S, Yu A, Zhang J. Handbook of clean energy systems. 2015. p. 1.

[3] Zhirnov VV, Cavin III RK. Microsystems for bioelectronics. The nanomorphic cell. Elsevier Inc; 2010.

[4] Scherson DA, Palencsár A. Batteries and electrochemical capacitors. The Electrochemical Society Interface, Spring; 2006. p. 17–22.

[5] Winter M, Brodd RJ. What are batteries, fuel cells, and supercapacitors. Chem Rev 2004;104:4245–69.

[6] Wang G, Dai AZ, Guan Y, Dong P, Wu L. Power management of hybrid power systems with Li-Fe batteries and supercapacitors for mobile robots. Adv Mech Eng 2014;2014:1–11.

[7] Song Z, Hou J, Hofmann H, Li J, Ouyang M. Sliding-mode and Lyapunov function-based control for battery/supercapacitor hybrid energy storage system used in electric vehicles. Energy 2017:601–12.

[8] Pushparaj VL, Sreekala S, Nalamasu O, Ajayan PM. Semiconductor nanomaterials for flexible technologies. Elsevier; 2010.

[9] Sh Hu, Rajamani R, Yu X. Flexible solid-state paper based carbon nanotube supercapacitor. Appl Phys Lett 2012;100. 104103–1-104103-4.

[10] Shi Sh, Xu Ch, Yang Ch, Li J, Du H, Li B, Kang F. Flexible supercapacitors. Particuology 2013;11:371–7.

[11] Simon P, Gogotsi Y. Materials for electrochemical capacitors. Nat Mater 2008;7:845–54.

[12] Senthilkumar ST, Kalai Selvan R, Ulaganathan M, Melo JS. Fabrication of Bi₂O₃|| AC asymmetric supercapacitor with redox additive aqueous electrolyte and its improved electrochemical performances. Electrochim Acta 2014;115:518–24.

[13] Shen C, Wang X, Li S, Wang J, Zhang W, Kang F. A high-energy-density micro supercapacitor of asymmetric MnO2–carbon configuration by using microfabrication technologies. J Power Sources 2013;234:302–9.

[14] Ganesh V, Pitchumani S, Lakshminarayanan V. New symmetric and asymmetric supercapacitors based on high surface area porous nickel and activated carbon. J Power Sources 2006;158:1523–32.

[15] Dubal DP, Jagadale AD, Lokhande ChD. Big as well as light weight portable, Mn₃O₄ based symmetric supercapacitive devices: fabrication, performance evaluation and demonstration. Electrochim Acta 2012;80:160–70.

[16] Xia H, Meng YSh, Yuan G, Ch Cui, Lu L. A symmetric RuO₂/RuO₂ supercapacitor operating at 1.6 V by using a neutral aqueous electrolyte. Electrochem Solid State Lett 2012;15:A60–3.

[17] Xie L-J, Wu J-F, Chen Ch-M, Zhang Ch-M, Wan L, Wang J-L, et al. A novel asymmetric supercapacitor with an activated carbon cathode and a reduced graphene oxide-cobalt oxide nanocomposite anode. J Power Sources 2013;242:148–56.

[18] Lia X, Wei B. Supercapacitors based on nanostructured carbon. Nano Energy 2013;2:159–73.

[19] Pandolfo AG, Hollenkamp AF. Carbon properties and their role in supercapacitors. J Power Sources 2006;157:11–27.

[20] Tiwari JN, Tiwari RN, Kim KS. Zero-dimensional, one-dimensional, two-dimensional and three-dimensional nanostructured materials for advanced electrochemical energy devices. Prog Mater Sci 2012;57:724–803.

[21] Kuzmenko V, Naboka O, Haque M, Staaf H, Göransson G, Gatenholm P, et al. Sustainable carbon nanofibers/nanotubes composites from cellulose as electrodes for supercapacitors. Energy 2015:1490–6.

[22] Wang K, Wu H, Meng Y, Wei Zh. Conducting polymer nanowire arrays for

high performance supercapacitors. Small 2014;10:14—31.

[23] Mi H, Zhang X, Yang S, Ye X, Luo J. Polyaniline nanofibers as the electrode material for supercapacitors. Mater Chem Phys 2008;112:127—31.

[24] Chee WK, Lim HN, Huang NM. Electrochemical properties of free-standing polypyrrole/graphene oxide/zinc oxide flexible supercapacitor. Int J Energy Res 2015;39:111—9.

[25] Yu G, Xie X, Pan L, Bao Z, Cui Y. Hybrid nanostructured materials for high-performance electrochemical capacitors. Nano Energy 2013;2:213—34.

[26] Mondal SK, Barai K, Munichandraiah N. High capacitance properties of poly-aniline by electrochemical deposition on a porous carbon substrate. Electro-chim Acta 2007;52:3258—64.

[27] Sieben JM, Morallón E, Cazorla-Amorós D. Flexible ruthenium oxide-activated carbon cloth composites prepared by simple electrodeposition methods. En-ergy 2013;58:519—26.

[28] Bavio MA, Acosta GG, Kessler T. Synthesis and characterization of polyaniline and polyaniline—carbon nanotubes nanostructures for electrochemical supercapacitors. J Power Sources 2014;245:475—81.

[29] Bavio MA, Acosta GG, Kessler T. Polyaniline and polyaniline—carbon black nanostructures as electrochemical capacitor electrode materials. Int J Hydrogen Energy 2014;39:8582—9.

[30] Cai JJ, Kong LB, Zhang J, Luo YCh, Kang L. A novel polyaniline/mesoporous carbon nano-composite electrode for asymmetric supercapacitor. Chin Chem Lett 2010;21:1509—12.

[31] Lee S-Y, Kim J-I, Park S-J. Activated carbon nanotubes/polyaniline composites as supercapacitor electrodes. Energy 2014;78:298—303.

[32] Gupta V, Miura N. Influence of the microstructure on the supercapacitive behavior of polyaniline/singlewall carbon nanotube composites. J Power Sources 2006;157:616—20.

[33] Fei H, Yang CH, Bao H, Wang G. Flexible all-solid state supercapacitors based on graphene/carbon black nanoparticle film electrodes and cross-linked pol-y(vinylalcohol)-H$_2$SO$_4$ porous gel electrolytes. J Power Sources 2014;266: 488—95.

[34] Shi CH, Zhao Q, Li H, Liao Z-M, Yu D. Low cost and flexible mesh-based supercapacitors for promising large-area flexible/wearable energy storage. Nano Energy 2014;6:82—91.

[35] Tehrani Z, Thomas DJ, Korochkina T, Phillips CO, Lupo D, Lehtimäki S, et al. Large-area printed supercapacitor technology for low-cost domestic green energy storage. Energy 2017;118:1313—21.

[36] Zujovic ZD, Laslau C, Bowmaker GA, Kilmartin PA, Webber AL, Brown SP, et al. Role of aniline oligomeric nanosheets in the formation of polyaniline nano-tubes. Macromolecules 2010;43:662—70.

[37] Zhou C, Han J, Guo R. Synthesis of polyaniline hierarchical structures in a dilute SDS/HCl solution: nanostructure covered rectangular tubes. Macro-molecules 2009;42:1252—7.

[38] Conway BE, Pell WG. Power limitations of supercapacitor operation associated with resistance and capacitance distribution in porous electrode devices. J Power Sources 2002;105:169—81.

[39] Bavio MA, Acosta GG, Kessler T. Energy storage in symmetric and asymmetric supercapacitors based in carbon cloth/polyaniline—carbon black nano-composites. Int J Energy Res 2015;39:2053—61.

[40] Cao Y, Lin B, Sun Y, Yang H, Zhang X. Symmetric/asymmetric supercapacitor based on the perovskite-type Lanthanum cobaltate nano fibers with Sr-sub-stitution. Electrochim Acta 2015;178:398—406.

[41] Shen J, Liu A, Tu Y, Foo G, Ch Yeo, Chan-Park MB, et al. How carboxylic groups improve the performance of single-walled carbon nanotube electrochemical capacitors? Energy & Environ Sci 2011;4:4220—9.